

## 반응압출 공정에 의한 사슬연장 Poly(D-lactide)의 합성 및 반응 동역학과 열적 분해 거동

Zhongbo Song and Weijun Zhen<sup>†</sup>

Key Laboratory of Oil and Gas Fine Chemicals, Ministry of Education and Xinjiang Uygur Autonomous Region,  
Xinjiang University

(2017년 2월 20일 접수, 2017년 5월 14일 수정, 2017년 6월 8일 채택)

## Preparation, the Chain-extending Reaction Kinetics and Thermal Degradation of Poly(D-lactide) by Reactive Extrusion Process

Zhongbo Song and Weijun Zhen<sup>†</sup>

Key Laboratory of Oil and Gas Fine Chemicals, Ministry of Education and Xinjiang Uygur Autonomous Region,  
Xinjiang University, Urumqi 830046, China

(Received February 20, 2017; Revised May 14, 2017; Accepted June 8, 2017)

**Abstract:** The chain-extended poly(D-lactide) (PDLA) was prepared from D-lactide under optimum polymerization conditions of 1 wt% stannous octoate, at 170 °C, 10 rpm for 15 min or 10 min with the addition of chain extender (4,4'-diphenylmethane diisocyanate (MDI), hexamethylene diisocyanate (HDI)) by reactive extrusion process. The molecular weight of PDLA-MDI and PDLA-HDI was 45376 and 47238 g/mol, respectively, which had been significantly improved compared with PDLA ( $M_w=20730$  g/mol). Furthermore, differential scanning calorimetry (DSC) results showed that the crystallinity of PDLA-MDI and PDLA-HDI was increased by 66.04 and 78.60%, respectively, compared with PDLA. Moreover, the rheological results and thermal decomposition kinetics results showed that the MDI and HDI had restricted the mobility of PDLA chains and enhanced the apparent activation energy ( $E_a$ ) of thermal degradation of PDLA.

**Keywords:** poly(D-lactide), reactive extrusion process, chain-extending, kinetics.

### Introduction

At present, the concept “green” reflects the need for sustainable materials and for environmental protection. A number of factors contribute to the success of polylactide (PLA) in these applications like in textiles, medical field, and also in the packaging industry<sup>1,2</sup> including its physical properties, favorable degradation characteristics, and benign degradation products.<sup>3</sup> However until now, PLA still has some disadvantages. For instance, slow crystallization rate, low crystalline degree and poor heat resistance of PLA have restricted its practical applications.<sup>4,5</sup> Therefore, it is very important to improve the crystallinity and properties of PLA by modification.<sup>6</sup> PLA is enantiomeric polyester including poly(L-lactide) (PLLA) and poly(D-lactide) (PDLA). One interesting attribute of PLA is

the ability of enantiomeric blends of PLLA and isotactic PDLA to form a kind of vertical crystal structure (SC)<sup>7-9</sup> with high crystal stability, thermal stability and mechanical properties. However, low molecular weight PDLA isolated in the matrix of PLLA did not form a stereocomplex crystallite with a surface area large enough to act as a nucleation site.<sup>10</sup> On the other hand, high molecular weight PDLA chains formed a large stereocomplex crystallite.<sup>10</sup> Thus, higher molecular weight of PDLA is desirable. Until now, high molecular weight PDLA was synthesized by ring-opening polymerization of the D-lactide,<sup>11</sup> which is relatively complicated and expensive. However, it is difficult to remove the water in order to obtain high molecular weight PDLA during ring-opening polymerization. When the reaction temperature was increased to remove the water, PDLA was easy to decompose at high temperature.<sup>12</sup> A large number of investigations have been made to improve PLA properties via plasticization, copolymerization, and blending with elastomers.<sup>13-15</sup> Among them, low-cost, 4,4'-diphenylmethane diisocyanate (MDI) and hexamethylene

<sup>†</sup>To whom correspondence should be addressed.

E-mail: zhenweijun6900@163.com

©2017 The Polymer Society of Korea. All rights reserved.

diisocyanate (HDI) as chain extender are the simplest and most effective choice. At present, reactive extrusion process has been received considerable attention as one kind of effective process because of the following advantages:<sup>16</sup> (1) It takes advantage of the high viscosities at advanced stages of polymerization to transfer through drag flow; (2) The extruder allows for good control of the reaction temperature by heat exchange through the barrel and screw surface; (3) The improved surface/volume ratio leads to higher conversion throughout the entire extruder channel.

The aim of this work was to obtain high molecular weight PDLA with the addition of chain extender MDI and HDI by the reactive extrusion process. We present the evaluation of reactive extrusion as a new process for the chain-extending reaction of PDLA and obtain the optimum technology parameters of chain extension with the addition of MDI and HDI based on reactive extrusion process. The properties of neat PDLA and chain extended PDLA with MDI and HDI were characterized through a series of tests. The chain extension reaction kinetics and thermal decomposition kinetics of PDLA based on the reactive extrusion process were studied.

## Experimental

**Materials.** D-lactide was purchased from Shenzhen Guanhuaweiye Industrial Co., Ltd., China. 4,4'-diphenylmethane diisocyanate (MDI, GR), hexamethylene diisocyanate (HDI, GR) and stannous octoate (AR) were purchased from J&K Scientific Ltd., China.

**Preparation of Chain-extended PDLA.** D-lactide and a specific amount of chain extender, these mixtures were manually fed into the sealed double-screw extruder (HAAKE MiniLab II, diameter 19 mm and L/D=25:1, Germany) melted at 120 °C under nitrogen atmosphere, and then a specific amount of the catalyst stannous octoate was added into the reaction process followed in cases at the set temperature and screw speed for several minutes under nitrogen atmosphere, and the obtained chain-extending samples were a white solid.

PDLA without chain extender was also processed with the same method. After these chain-extending PDLA were extruded and pelletized, the samples were injection molded (HAAKE Mini Jet pro) into standard test specimens for tensile, and impact tests. During injection molding, all samples were molded under 70 MPa pressure at 180 °C, mold temperature of 50 °C and pressure-holding time of 10 s.

**Characterization.** Gel permeation chromatography (GPC)

was conducted using an Agilent 1100 Gel Permeation Chromatograph (USA). The solvent was tetrahydrofuran, with a flow rate of 0.6 mL/min. The injection volume was 10  $\mu$ L and column temperature was 40 °C.

<sup>1</sup>H nuclear magnetic resonance spectroscopy (<sup>1</sup>H NMR) were recorded on an Inova 400 MHz spectrometer (Varian, Co., Ltd., USA) at 400 MHz in dimethyl sulfoxide (DMSO-*d*<sub>6</sub>) at room temperature.

Fourier transform infrared spectroscopy (FTIR) of the samples was carried out on a Bruker-Equinox 55 (Germany) spectrometer using standard KBr pellet/disc technique. Spectra were recorded over a spectral range of 4000 to 400  $\text{cm}^{-1}$  with a resolution of 4  $\text{cm}^{-1}$ .

Tensile tests were carried out according to ASTM D 412-80 using Instron 4302 Universal Testing Machine (USA) at a cross head speed of 5 mm/min. At least five measurements for every sample were made. Samples of PLLA composites were standard test specimens from the injection mold.

Notched izod impact testing was carried out using a Testing Machines Inc. 43-02-01 Monitor/Impact machine (USA) according to ASTM D256. 2-mm-deep notches were cut into sample beams using a TMI notch cutter. All results presented were the average values of five measurements.

Scanning electron microscopy (SEM) (Inspect F, FEI Instrument Co., Ltd., Netherlands) at 20 kV of accelerating voltage was employed to study the impact fracture morphology. The composite samples were cooled in liquid nitrogen, and then fractured. Prior to SEM analysis, the samples were sputter coated with gold to prevent charging during the tests.

Thermal gravimetric analysis (TGA) was conducted on SDT-Q600 thermogravimetric analyzer (USA). Each sample (about 5-10 mg) was heated at a heating rate of 10 °C/min in the temperature range of room temperature to 500 °C under nitrogen flow (100 mL/min).

Differential scanning calorimetry (DSC) of each sample (about 5-8 mg) was conducted on DSC Q2000 differential scanning calorimeter (USA). Samples were heated from 20 to 200 °C at a heating rate of 10 °C/min under nitrogen flow (50 mL/min).

The rheological behavior of all samples were characterized using a stress-controlled rotational rheometer (AR2000ex, TA Instruments) with 25 mm diameter and 1 mm gap parallel plates. Before the measurement, each disk-shaped specimen prepared by compression molding was heated to 170 °C and held for 3 min to completely melt PLA and nucleating agents. Deformation in the linear viscoelastic region was found to be

2% and then chosen for all subsequent frequency sweep tests. Samples were equilibrated at 170 °C before testing. The frequency was varied from 0.1 to 100 rad/s.

The capillary rheological behaviors of all samples were studied using HAAKE Mini LabII (diameter 19 mm and L/D=25:1, Germany). These samples (5~7 g) were manually fed into HAAKE Mini LabII at a temperature of 180 °C and the shearing rate varied from 1~50 rpm.

## Results and Discussion

**Orthogonal Experiment Analysis.** Orthogonal experiments were designed to investigate the most suitable reaction conditions, the factors and levels of which were listed in Table 1, in which the weight-average molecular weight ( $M_w$ ) of chain-extended was set as target function.

Results of the orthogonal experiment were shown in Table 2, which was used to investigate the effects of polymerization temperature, screw speed, amount of chain extender and residence time on the preparation of chain-extended PDLA. As shown in Table 2, the optimum conditions were found to be as follows: PDLA-MDI (170 °C, 10 rpm, 5 wt%, 15 min); PDLA-HDI (170 °C, 10 rpm, 5 wt%, 10 min). The molecular weight were increased with the addition of chain extender under optimum conditions compared with neat PDLA ( $M_w=20730$  g/mol). This was mainly due to fact that the nature of chain extension reaction was nucleophilic addition reaction for these two chain extenders. In addition, the effect of HDI was better than that of MDI, which was owing to HDI molecular chain with good activity and the structure of six methylene connecting with -NCO, which was similar with PDLA molecular chain.

**GPC Analysis.** Figure 1 shows the GPC curves for PDLA before and after chain extending. The parameters of the GPC analysis results were listed in Table 3. The GPC results showed that the retention time for PDLA before and after chain extending under optimum reaction conditions, the weight-average molecular weight ( $M_w$ ) was 20730 g/mol for PDLA, 45376 g/

mol for PDLA-MDI and 47238 g/mol for PDLA-HDI.

Additionally, the polydispersity index (PDI) was 1.724 for PDLA, 1.512 for PDLA-MDI and 1.573 for PDLA-HDI, respectively. The results suggested that PDLA before and after chain extending were a copolymer, rather than each monomer forming homopolymers or a hybrid homopolymer, and the chain extender connects the hydroxyl end group so as to increase the molecular weight.<sup>12</sup> This confirmed the successful obtain high molecular weight PDLA with the addition of chain extender MDI and HDI by the reactive extrusion process, which also supported the FTIR and <sup>1</sup>H NMR results.

**<sup>1</sup>H NMR Analysis.** The products of PDLA before and after chain extending were characterized by <sup>1</sup>H NMR (Figure 2). Figure 2(a) shows peaks at 1.6 and 5 ppm, which attributed to the existence of the structure of -CH<sub>3</sub> and -CH groups. The signal of the three equivalent H of the -CH<sub>3</sub> was splitting due to the H of -CH nearby and vice versa.

This is caused by electrostatic shield effect produced from the end hydroxyl groups in PDLA chains.<sup>17</sup> The ratio of the areas of the two peaks was 3:1, which was consistent with the ratio of the number of hydrogens along the PDLA chain. Figure 2(b) and 2(c) shows peak at 7.52 ppm, which attributed to the introduction of MDI and HDI chain extender products proton absorption peak. Peak at 3.75 ppm, which was due to the introduction of chain extender different NH proton absorption.

This confirmed the successful coupling reaction between the -NCO group of MDI and HDI with the -OH of PDLA, which also supported the FTIR results.

**FTIR Analysis.** FTIR analysis has been widely used to identify the interactions and phase behavior of polymer composites. The spectrum of PDLA before and after chain extending in the region from 400 to 4000 cm<sup>-1</sup> is presented in Figure 3. In the FTIR spectrum of PDLA, the O-H bending and stretching vibrations of PDLA appeared at 3330-3600 cm<sup>-1</sup>. The band due to C=O stretching vibration of carbonyl appeared at 1758 cm<sup>-1</sup>.<sup>18</sup> The peaks at 2946 to 2999 cm<sup>-1</sup> could be attributed to the asymmetric stretching vibrations of C-H, whereas the peak at 1,448 cm<sup>-1</sup> was attributed to the defor-

**Table 1. Factors of Levels of the Orthogonal Experiment**

| Level | Factor | (A) Polymerization temperature (°C) | (B) Screw speed (rpm) | (C) Amount of chain extender (wt%) | (D) Residence time (min) |
|-------|--------|-------------------------------------|-----------------------|------------------------------------|--------------------------|
| 1     |        | 150                                 | 5                     | 1                                  | 5                        |
| 2     |        | 160                                 | 10                    | 3                                  | 10                       |
| 3     |        | 170                                 | 15                    | 5                                  | 15                       |
| 4     |        | 180                                 | 20                    | 7                                  | 20                       |

**Table 2. Results of the Orthogonal Experiment**

| Test number | Factor | (A) (°C) | (B) (rpm) | (C) (wt%) | (D) (min) | PDLA-MDI $M_w$ (g/mol) | PDLA-HDI $M_w$ (g/mol) |
|-------------|--------|----------|-----------|-----------|-----------|------------------------|------------------------|
| 1           |        | 150      | 5         | 1         | 5         | 16942                  | 18301                  |
| 2           |        | 150      | 10        | 3         | 10        | 19954                  | 22349                  |
| 3           |        | 150      | 15        | 5         | 15        | 24531                  | 26304                  |
| 4           |        | 150      | 20        | 7         | 20        | 20730                  | 23079                  |
| 5           |        | 160      | 5         | 5         | 10        | 25546                  | 27950                  |
| 6           |        | 160      | 10        | 7         | 5         | 24596                  | 26285                  |
| 7           |        | 160      | 15        | 1         | 20        | 20124                  | 22042                  |
| 8           |        | 160      | 20        | 3         | 15        | 23302                  | 21173                  |
| 9           |        | 170      | 5         | 7         | 15        | 25886                  | 24529                  |
| 10          |        | 170      | 10        | 5         | 20        | 35447                  | 36630                  |
| 11          |        | 170      | 15        | 3         | 5         | 26527                  | 29190                  |
| 12          |        | 170      | 20        | 1         | 10        | 30865                  | 34064                  |
| 13          |        | 180      | 5         | 3         | 20        | 20323                  | 22492                  |
| 14          |        | 180      | 10        | 1         | 15        | 25174                  | 25595                  |
| 15          |        | 180      | 15        | 7         | 10        | 22362                  | 24747                  |
| 16          |        | 180      | 20        | 5         | 5         | 25942                  | 28263                  |
| <hr/>       |        |          |           |           |           |                        |                        |
| PDLA-       | K1     | 20539    | 22174     | 23276     | 23502     |                        |                        |
| MDI         | K2     | 23392    | 26293     | 22527     | 24682     |                        |                        |
|             | K3     | 29681    | 23386     | 27866     | 24723     |                        |                        |
|             | K4     | 23450    | 25210     | 23394     | 24156     |                        |                        |
|             | R      | 9142     | 4118      | 5340      | 1222      |                        |                        |
| <hr/>       |        |          |           |           |           |                        |                        |
| PDLA-       | K1     | 22508    | 23318     | 25001     | 25510     |                        |                        |
| HDI         | K2     | 24363    | 27714     | 23801     | 27278     |                        |                        |
|             | K3     | 31103    | 25571     | 29787     | 24400     |                        |                        |
|             | K4     | 25274    | 26645     | 24660     | 26061     |                        |                        |
|             | R      | 8595     | 4397      | 5986      | 2877      |                        |                        |

The effects of factors on experimental results:  $A > C > B > D$ .

Optimum conditions: PDLA-MDI (170 °C, 10 rpm, 5 wt%, 15 min); PDLA-HDI (170 °C, 10 rpm, 5 wt%, 10 min).

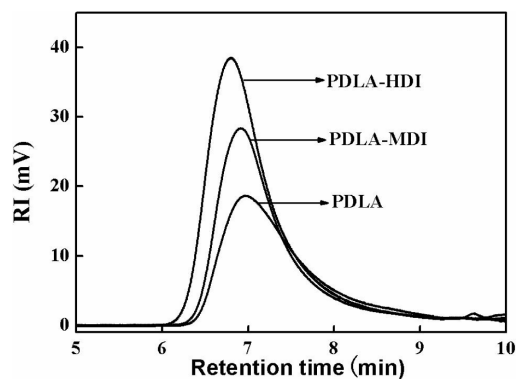


**Figure 1.** GPC measurement of PDLA before and after chain extending.

mation of C-H in the  $\text{CH}_3$  group. The peak of stretching vibration of C-O and C-O-C occurred at 1214 and 1095  $\text{cm}^{-1}$ . Both the two characteristics proved the presence of the terminal hydroxyl groups and ester groups in the chain of PDLA. The peak corresponding to C-C single bond appeared at 920 and 871  $\text{cm}^{-1}$ .<sup>19</sup> The FTIR spectra of PDLA before and after chain extending were consistent. It was evident that the addition of chain extender did not change the molecular chains structure of PDLA.

The peak of stretching vibration of  $-\text{NH}_2$  occurred at 3379 and 1523  $\text{cm}^{-1}$ , which indicated that the  $-\text{NH}_2$  was introduced during chain extension process. The peak became more strong

**Table 3. Results of the GPC of PDLA before and after Chain Extending**

| Sample   | $M_n$ | $M_w$ | $M_z$ | $M_z/M_w$ | $M_w/M_n$ |
|----------|-------|-------|-------|-----------|-----------|
| PDLA     | 12024 | 20730 | 38869 | 1.875     | 1.724     |
| PDLA-MDI | 30010 | 45376 | 80134 | 1.766     | 1.512     |
| PDLA-HDI | 30030 | 47238 | 85217 | 1.804     | 1.573     |

and sharp at  $1758\text{ cm}^{-1}$ , which was due to the introduction of ester base into PDLA molecular chains. However, the peak of stretching vibration of -NCO- groups did not occur at  $2200\text{--}2300\text{ cm}^{-1}$ , and this stated that the groups of -NCO- and -OH were react sufficiently during chain extending process.

**Mechanical Performance of Chain Extended PDLA.** The effects of chain extender on the mechanical properties of pure PDLA were shown in Figure 4. It was evident that the incorporation of chain extender slightly improved the tensile strength and the elongation at break compared with pure PDLA.<sup>21</sup>

Figure 4 clearly showed that the maximum tensile strength and elongation at break of PDLA-MDI had been increased by 15.83 and 3.08%, and the maximum tensile strength and elongation at break of PDLA-HDI had been increased by 19.64 and 3.80% compared with PDLA. Consequently, the tensile strength and elongation at break of PDLA with chain extenders were increased. Moreover, the impact strength of PDLA-MDI and PDLA-HDI was increased by 47.43 and 71.57% compared with PDLA, and the impact strength is the characterization of resistance to high pressure caused by rupture of ability, direct relationship between the material toughness.<sup>20</sup> This indicated that the addition of chain extender significantly modified the mechanical performance of PDLA.<sup>21</sup> These were also in good accordance with the DSC results.

**Thermogravimetric Analysis (TGA).** Thermogravimetric analysis (TGA) was conducted to investigate the thermal properties of PDLA before and after chain extending. Figure 5 shows the TG-DTG curves of pure PDLA and PDLA with chain extender. The decomposition temperature ( $T_d$ ) of pure PDLA was  $294\text{ }^\circ\text{C}$ , whereas in case of PDLA with chain extender,  $T_d$  was  $307\text{ }^\circ\text{C}$  for PDLA-MDI and  $318\text{ }^\circ\text{C}$  for PDLA-HDI, respectively. This indicated an improvement in the thermal stability of the chain extended PDLA. It was interesting to note that PDLA-HDI displayed the highest decomposition temperatures, which was increased by  $24\text{ }^\circ\text{C}$ , and  $T_d$  of PDLA-MDI was increased by  $13\text{ }^\circ\text{C}$ . The current results indicated the effect of chain extender, which improved the thermal stability. High molecular weight of PDLA-MDI and PDLA-

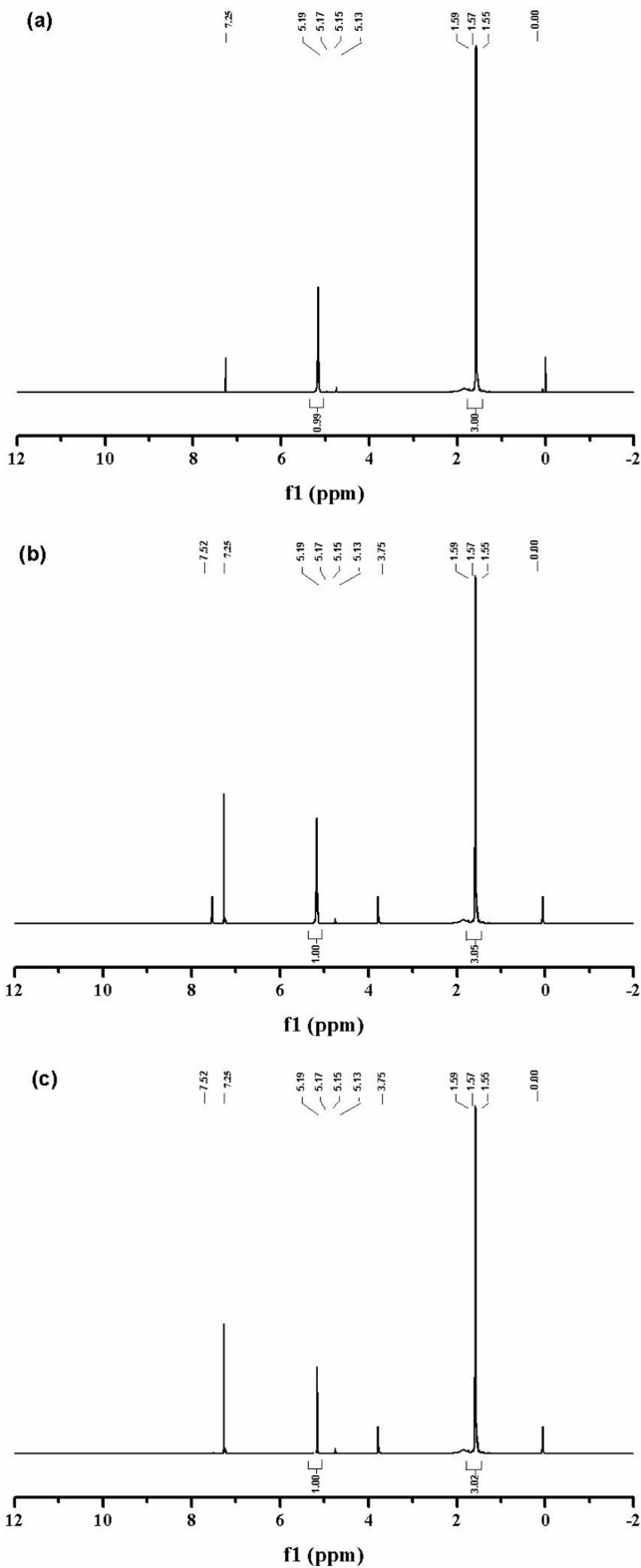
HDI showed a higher viscosity during temperature rising process, and increased the forces between molecular chains.

Moreover, the introduction of benzene ring and amide group also improved the thermal stability of PDLA.<sup>22</sup>

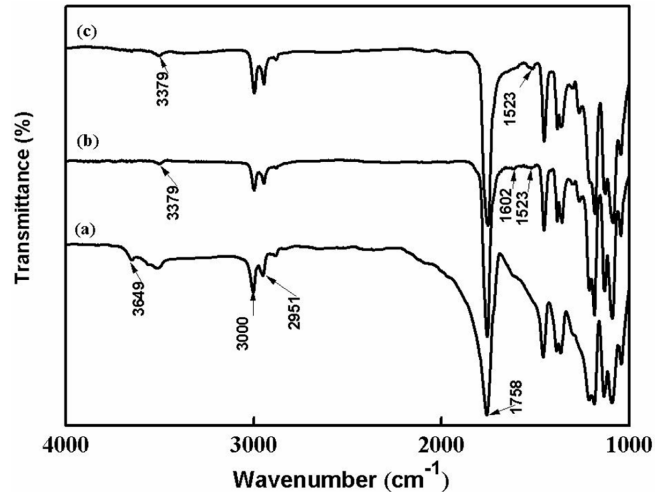
**Differential Scanning Calorimetry (DSC).** Variations in thermal transitions provide useful information regarding the physical structure of material. Figure 6 shows the DSC curves of PDLA before and after chain extending. Crystallinity of the polymer could be calculated by the formula:  $X_c = \{(\Delta H_m - \Delta H_c)/(f \cdot \Delta H_m^0)\} \cdot 100\%$ ,<sup>23</sup> where  $\Delta H_m^0$  is the melting enthalpy, expected for polymer with 100% crystallinity. The melting enthalpy ( $\Delta H_m$ ), and the relative crystallinity ( $X_c$ ), defined by the ratio of  $\Delta H_c$  to the heat of fusion of the purely crystalline form of PLA. The heat of fusion  $\Delta H_m^0$  is  $93.7\text{ J/g}$ ,<sup>24</sup> and  $f$  is weight factor of PDLA.

Table 4 shows the DSC feature values of PDLA before and after chain extending. From the DSC curves, it was shown that the cold crystallization disappeared after introduction of MDI and HDI. The values of  $T_m$  tended towards the high temperature region. This change of behavior was due to chain extender, which improved the crystallinity of PDLA-MDI and PDLA-HDI compared to PDLA. Table 4 showed the crystallinities of PDLA, PDLA-MDI and PDLA-HDI were 8.50, 26.80, and 31.34%, respectively. The crystallinities of PDLA-MDI and PDLA-HDI had been significantly improved, which was resulted from the improved of molecular weight of PDLA, and the isocyanate groups of chain extender could form urethane bonds with the hydroxyl end groups of PDLA molecules,<sup>21</sup> which increased the forces between molecular chains. This result was further in good accordance with the mechanical testing results.

**Morphological Analysis.** SEM analysis of the fractured surfaces of PDLA before and after chain extending were shown in Figure 7, which confirmed the effect of addition of chain extender on the mechanical behavior of the material. The samples were cooled in liquid nitrogen, and then fractured after mechanical tests and the fractured surfaces were quite different. Pure PDLA showed a typical brittle fracture, which had only a few shear zones initiated and led to low toughness and



**Figure 2.** <sup>1</sup>H NMR spectra of PDLA before and after chain extending: (a) PDLA; (b) PDLA-MDI; (c) PDLA-HDI.



**Figure 3.** FTIR spectra of PDLA before and after chain extending: (a) PDLA; (b) PDLA-MDI; (c) PDLA-HDI.

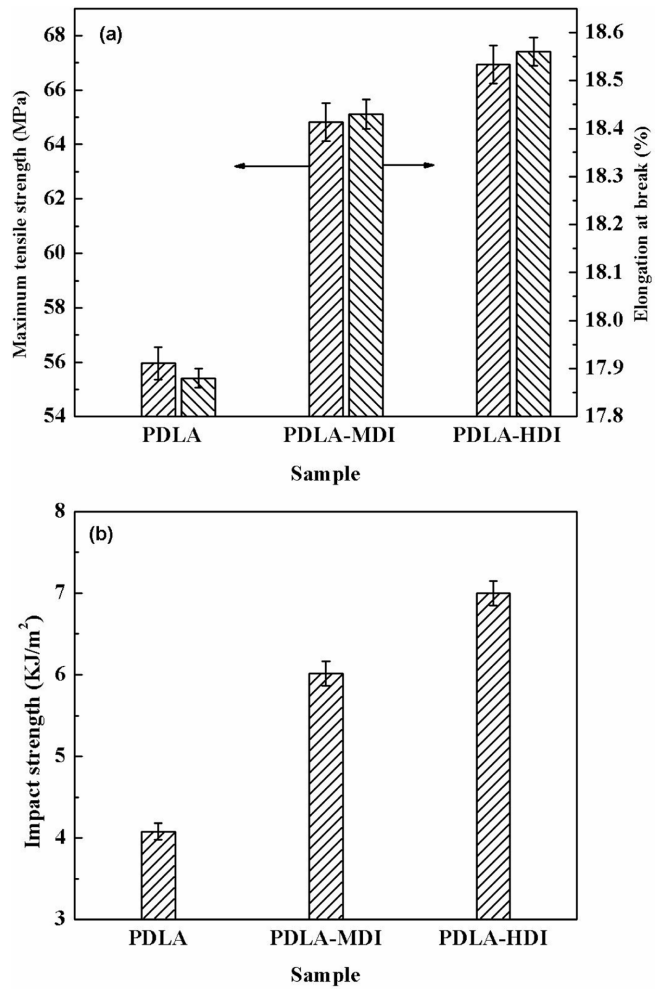


**Figure 4.** Effects of chain extender on mechanical properties of PDLA: (a) Maximum tensile strength and elongation at break; (b) Impact strength.

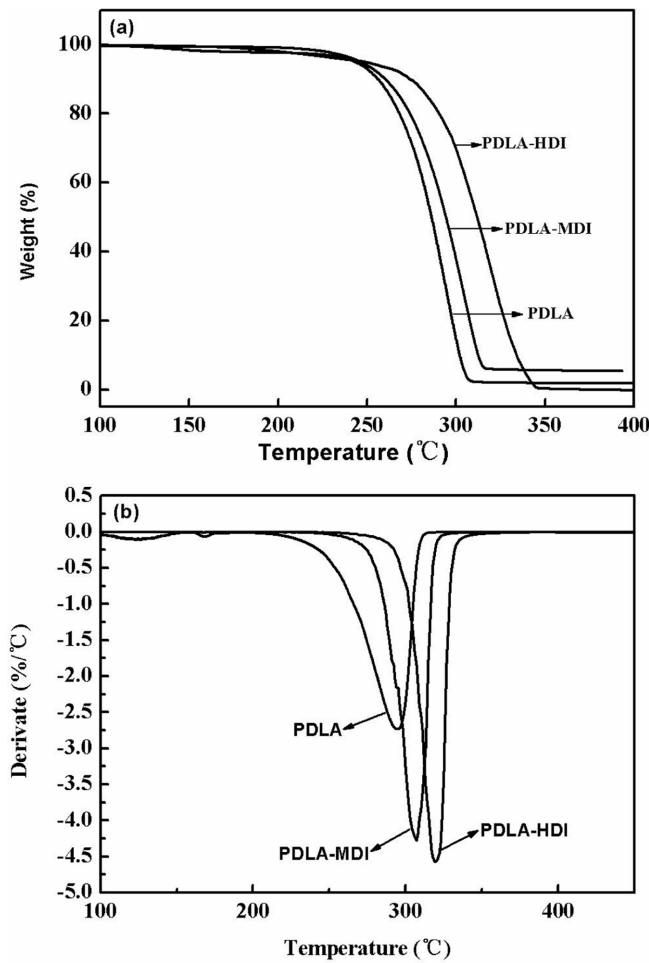


**Figure 5.** TGA curves of PDLA before and after chain extending: (a) TG; (b) DTG.

shock strength. However, more shear zones and fibrillations were observed on the surfaces of PDLA-MDI and PDLA-HDI, which contributed to the improvement of toughness and plastic deformation occurred during the test. This ascribed to the improved of molecular weight of PDLA, and the isocyanate groups of chain extender could form urethane bonds with the hydroxyl end groups of PDLA molecules,<sup>21</sup> which increased the forces between molecular chains, and which was benefited for absorbing more impact energy during impact test.<sup>25</sup> This was consistent with the results of mechanical testing.

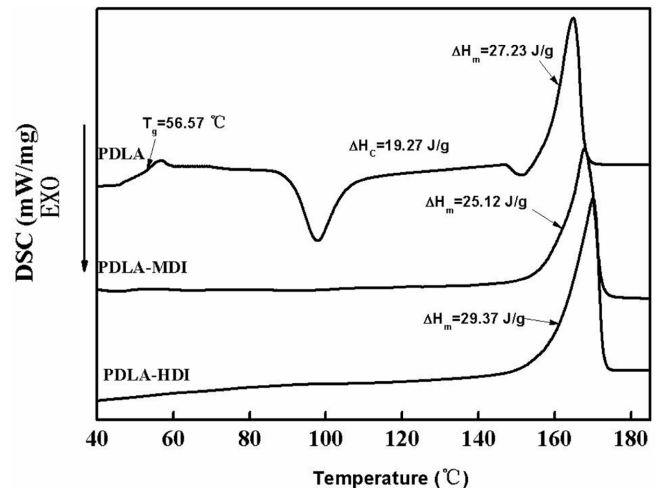


**Figure 6.** DSC curves of PDLA before and after chain extending.

**Chain Extension Reaction Kinetic Analysis.** To simplify the PDLA chain extension reaction kinetic model, the reaction between -NCO and -OH was only considered, and other reactions were ignored.

According to the mechanism of chain extension reaction, PDLA chain extension reaction rate can be used the concentration change rate of the end groups (-NCO and -OH). Thus the chain extension reaction rate equation can be expressed as the formula (1).

$$r = -\frac{dc}{dt} = 2kc_{NCO}c_{OH} \quad (1)$$

The same amount of -NCO and -OH groups reacted sufficiently during chain extending process. The chain extension reaction rate equation was changed as the formula (2).

$$r = -\frac{dc}{dt} = 2kc^2 \quad (2)$$

Because the chain extension reaction was under the constant temperature condition without emissions and loss of material, so we supposed the volume of reaction solution did not change over time. The concentration of the reactants can use the quality as the benchmark (g/mol). According to the definition of

**Table 4.** DSC Feature Values of PDLA before and after Chain Extending

| Sample   | $T_g$ (°C) | $T_c$ (°C) | $T_m$ (°C) | $\Delta H_c$ (J/g) | $\Delta H_m$ (J/g) | $X_c$ (%) |
|----------|------------|------------|------------|--------------------|--------------------|-----------|
| PDLA     | 56.57      | 98.5       | 165.21     | 19.27              | 27.23              | 8.50      |
| PDLA-MDI | -          | -          | 168.73     | -                  | 25.12              | 26.80     |
| PDLA-HDI | -          | -          | 172.14     | -                  | 29.37              | 31.34     |

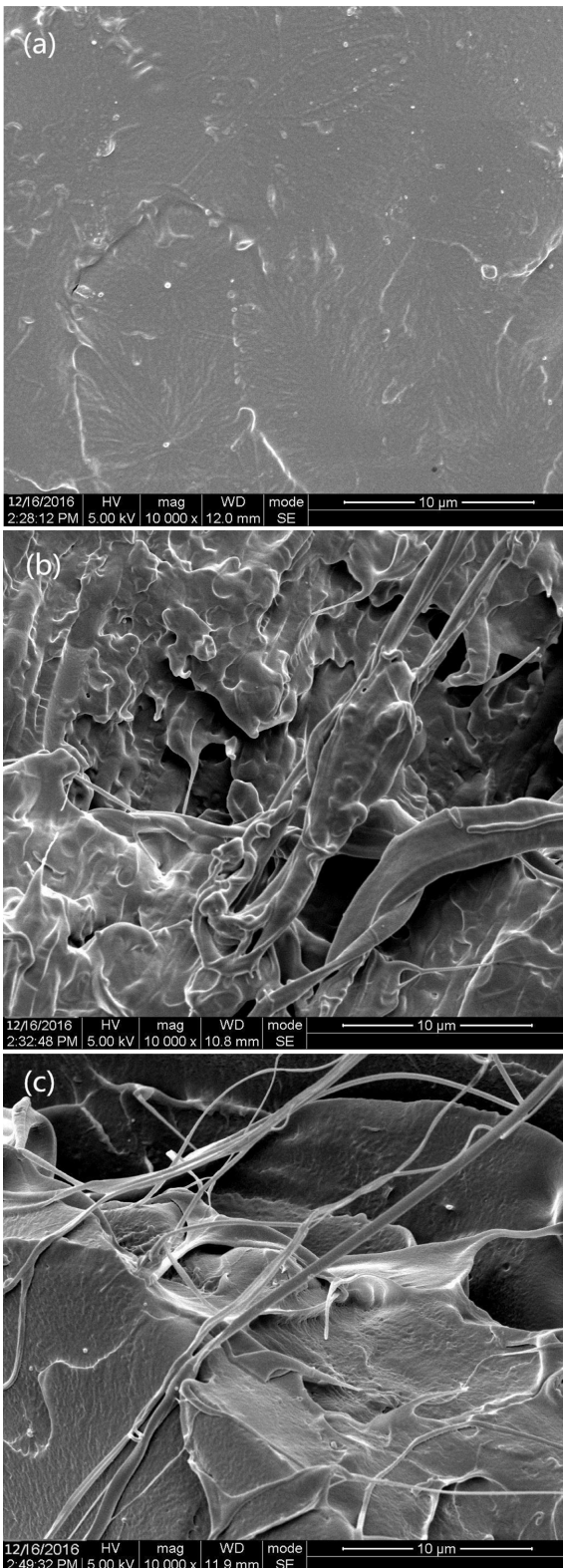


**Figure 7.** SEM morphology of fracture of PDLA before and after chain extending: (a) PDLA; (b) PDLA-MDI; (c) PDLA-HDI.

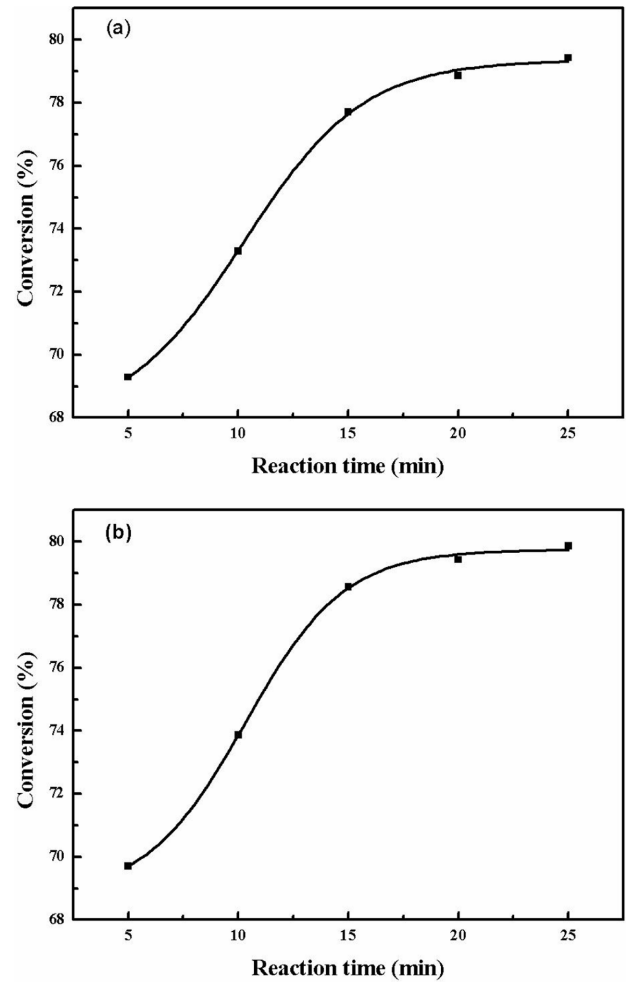


**Figure 8.** The relationship between reaction time and conversion: (a) PDLA-MDI; (b) PDLA-HDI.

the reactant conversion (2), the equation can be expressed as the formula (3).

$$\frac{x}{1-x} = 2kc_0t \quad (3)$$

Rewrite the formula (3) as (4) with the supposed of  $k' = 4k/M_n$  ( $c_0 = 2/M_n$ ).

$$\frac{x}{1-x} = k't \quad (4)$$

Figure 8 shows the relationship between reaction time and conversion. And then the linear fitting curves with  $x/1-x$  vs  $t$  were shown in Figure 9. From Figure 9, it was clear that MDI and HDI had good linear relationship to the chain extension reaction kinetics of PDLA, the linear fitting of  $R^2$  was respec-

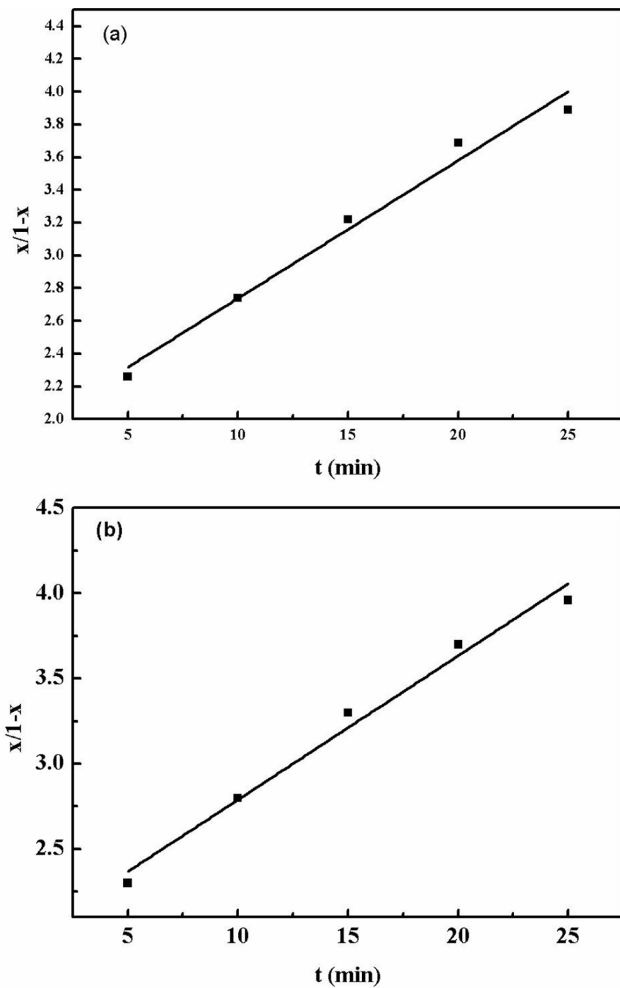


**Figure 9.** Linear plots of  $x/1-x$  vs  $t$ : (a) PDLA-MDI; (b) PDLA-HDI.

tively 0.987 for (a) and 0.991 for (b). Through the slope to calculated  $k'$ , and then obtained the apparent reaction rate constants of PDLA-MDI and PDLA-HDI were  $3.024 \times 10^3$  ( $\text{g} \cdot \text{mol}^{-1} \cdot \text{min}^{-1}$ ) and  $3.719 \times 10^3$  ( $\text{g} \cdot \text{mol}^{-1} \cdot \text{min}^{-1}$ ), which indicated that the chain extension speed was faster, chain extension time was shorter compared with MDI. HDI is one kind of small molecular weight organic liquid matter, so it can make the -NCO and -OH group quickly react. However, MDI has high relative molecular weight, and its molecular activity ability is poor and the introduction of rigid benzene ring to increase the difficulty of the molecular chain movement, which restrains the proceed of chain extension reaction. Therefore, the chain extension effect of HDI is better than that of MDI.

**Rheological Behavior Analysis.** Figure 10 shows storage modulus and complex viscosity as a function of frequency for PDLA before and after chain extending. On addition of MDI

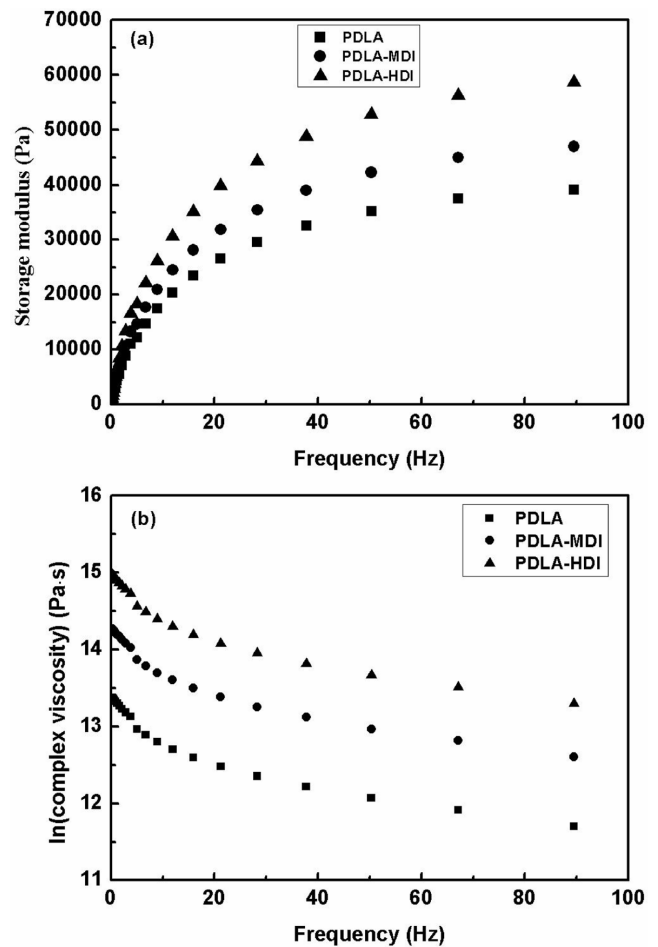


**Figure 10.** Rheological behavior of PDLA before and after chain extending: (a) Storage modulus; (b)  $\ln(\text{complex viscosity})$ .

and HDI, storage modulus (Figure 10(a)) showed a large increase in the frequency range of 0-40 Hz. On the other hand, it did not show a visible change at relatively high frequencies, which indicated that the composites definitely had the properties of viscoelastic materials. The dependency of frequency on the complex viscosity for all samples were shown in Figure 10(b). On addition of chain extender, viscosity of the blend decreased and the shear-thinning behavior intensified with increasing frequency. The storage modulus and complex viscosity of PDLA after chain extending were increased obviously compared with pure PDLA. The results were ascribed to the improved of molecular weight of PDLA, and the isocyanate groups of chain extender could form urethane bonds with the hydroxyl end groups of PDLA molecules,<sup>21</sup> which increased the forces between molecular chains and restricted the mobility of PDLA chains. The storage modulus and viscosity of PDLA extended by HDI were increased more than that of PDLA

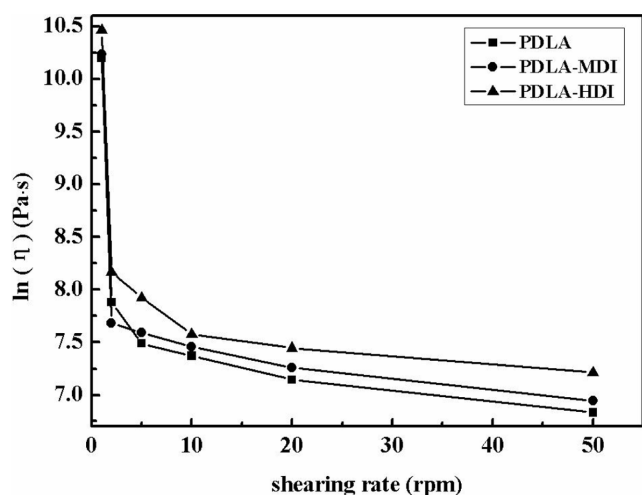
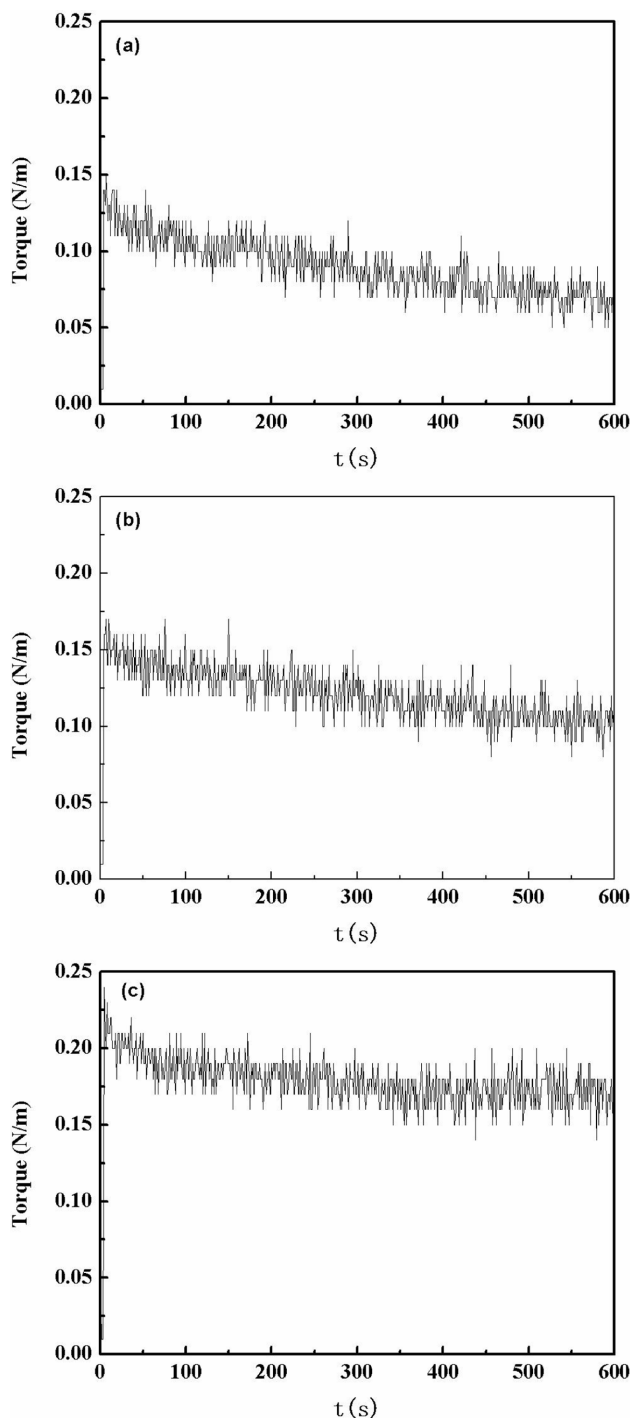


**Figure 11.**  $\ln(\eta)$ -shearing rate curves of PDLA before and after chain extending.

extended by MDI, which also was in good accordance with the chain extension reaction kinetics results.

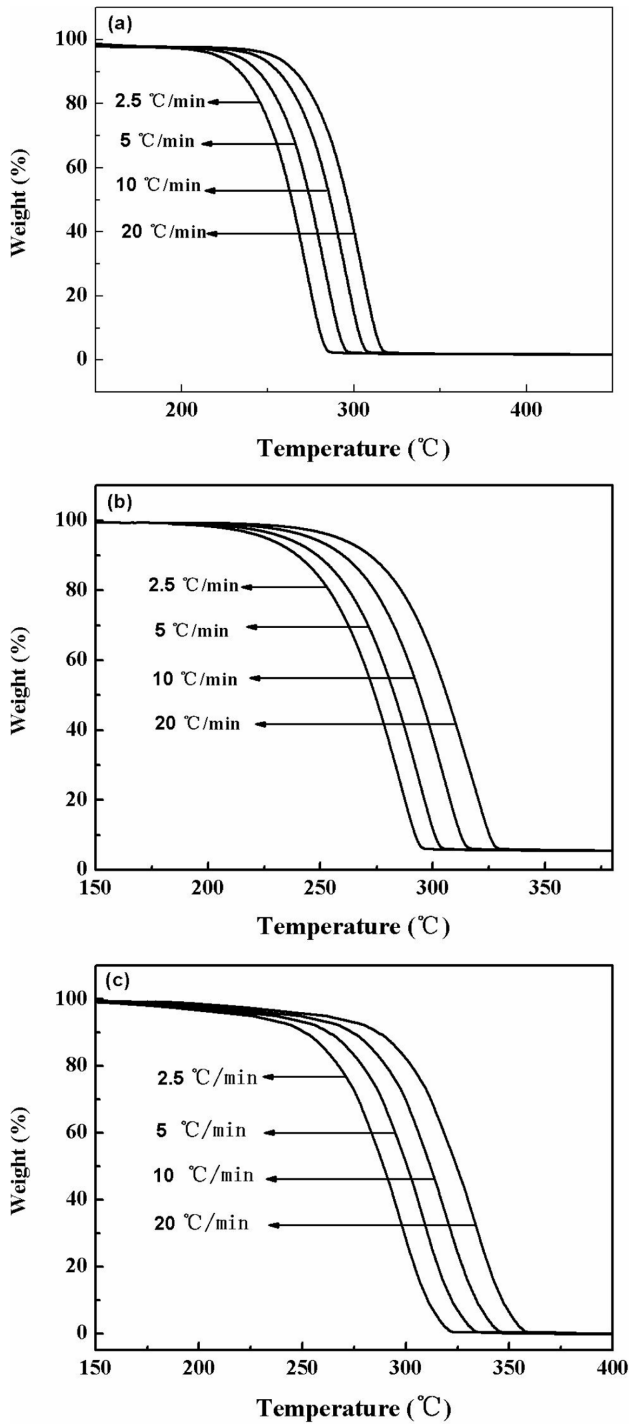
**Capillary Rheological Analysis.** Figure 11 shows  $\ln(\eta)$ -shearing rate curves of PDLA before and after chain extending. In Figure 11, the samples were showed uniform changes in their trends, in which the apparent viscosity decreased with increasing shearing rate at a constant temperature (180 °C). On addition of chain extender, the apparent viscosity was increased compared with pure PDLA. The results were ascribed to the improvement of molecular weight of PDLA, and the end groups of their molecules could be extended or connected with each other during the reaction extrusion,<sup>21</sup> which increased the forces between molecular chains and restricted the mobility of PDLA chains.<sup>26</sup> Moreover, HDI had the excellent effect than MDI on the chain extension of PDLA, which also was consistent with the results of chain extension reaction kinetics.

Figure 12 shows torque- $t$  curves of PDLA before and after chain extending. From Figure 12, it can be seen that flexible molecular chains of the samples easily tangle in melt at zero shear rate, while the shearing is favorable for disentanglement of the tangled chain and led to a certain extent of orientation, causing the melt viscosity to decrease obviously with the increase of shear rate,<sup>26</sup> and the torque increased dramatically in a short time, which was resulted from the increasing resistance in internal mixer chamber. The sample was broken up and began to melt under the shearing action of the twin screw, with further melting of the material, the resistance gradually reduced and torque decreased accordingly. The torque of PDLA before and after chain extending showed a downward



**Figure 12.** Torque- $t$  curves of PDLA before and after chain extending: (a) PDLA; (b) PDLA-MDI; (c) PDLA-HDI.

trend overall. The torque of PDLA-MDI and PDLA-HDI were higher than that of PDLA, which was the reason that the improvement of molecular weight of PDLA, and the enhancement of the end groups between chain extender and PDLA



**Figure 13.** TG curves of PDLA before and after chain extending: (a) PDLA; (b) PDLA-MDI; (c) PDLA-HDI.

molecular chains.<sup>21</sup> Thus the forces of PDLA chains had increased and the mobility was restricted.<sup>26</sup> The results were also correspond to Figure 11.

**Thermal Degradation Kinetic Analysis.** Figure 13 and

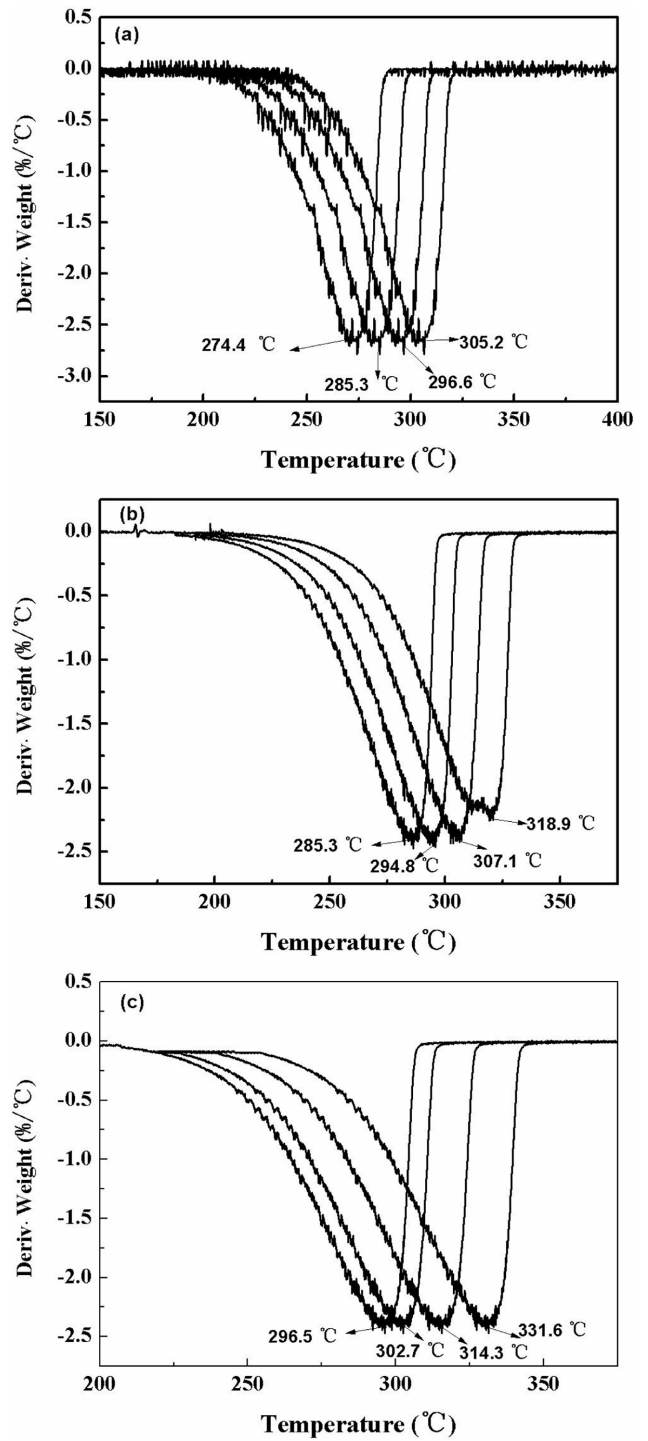


**Figure 14.** DTG curves of PDLA before and after chain extending: (a) PDLA; (b) PDLA-MDI; (c) PDLA-HDI.

Figure 14 shows TG and DTG curves of PDLA before and after chain extending at different heating rates. When the temperature was less than 200 °C, the weight loss of PDLA before and after chain extending were about 2%, which was mainly

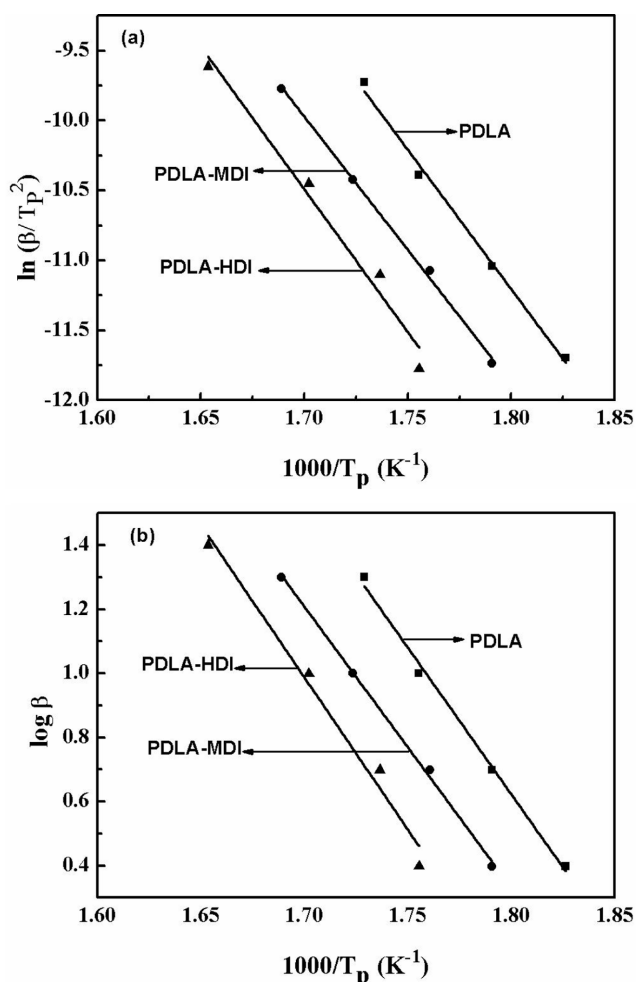


**Figure 15.** The graphs of thermal degradation kinetic data by Kissinger and Ozawa methods: (a) Kissinger; (b) Ozawa.

due to the steamed out of moisture at this stage. However, when the temperature exceeded 200 °C, the PDLA before and after chain extending began to appear fast pyrolysis, and with the increase of heating rate, the maximum weight loss temperature ( $T_p$ ) tended towards the higher temperature region. This is because the increase of heating rate makes the thermal degradation time shortened under the same temperature, and pyrolysis produces H<sub>2</sub>O and CO<sub>2</sub> releasing lag. In contrast,  $T_p$  of PDLA-MDI and PDLA-HDI were always higher than that of PDLA at the same heating rate, which indicated the effect of chain extender had improved the thermal stability. High molecular weight of PDLA-MDI and PDLA-HDI showed a higher viscosity during temperature rising process, and increased the forces between molecular chains. Moreover, the increasing of molecular weight of PDLA, and the isocyanate groups of chain extender could form urethane bonds with the hydroxyl

**Table 5. Thermal Degradation Kinetics Data of PDLA before and after Chain Extending**

| Samples  | Methods   | $E_a$ (KJ/mol) | $R^2$ |
|----------|-----------|----------------|-------|
| PDLA     | Kissinger | 153.48         | 0.992 |
|          | Ozawa     | 155.24         | 0.992 |
| PDLA-MDI | Kissinger | 158.55         | 0.997 |
|          | Ozawa     | 159.87         | 0.997 |
| PDLA-HDI | Kissinger | 165.84         | 0.987 |
|          | Ozawa     | 166.59         | 0.987 |

end groups of PDLA molecules, which improved the thermal stability of PDLA.<sup>21</sup>

Kissinger differential method<sup>27</sup> and Ozawa integral method<sup>28</sup> were used to estimate the apparent activation energy ( $E_a$ ) of PDLA before and after chain extending. The formula for the Kissinger method is expressed as the formula (5).

$$\ln\left(\frac{\beta}{T_p^2}\right) = \ln\left(\frac{AR}{E_a}\right) - \frac{E_a}{RT_p} \quad (5)$$

where  $\beta$  is the heating rate,  $A$  is frequency factor (s<sup>-1</sup>),  $R$  is ideal gas constant (8.314 J·mol<sup>-1</sup>·K<sup>-1</sup>). Figure 15(a) shows the graphs of thermal degradation kinetics data by Kissinger method. The formula can be deduced that  $\ln\left(\frac{\beta}{T_p^2}\right)$  proportional to  $\frac{1}{T_p}$ , so we can calculated  $E_a$  by the slope ( $-E_a/R$ ).

The formula for the Ozawa method is expressed as the formula (6).

$$\log \beta = \log \frac{AE_a}{RF(\alpha)} - 2.31 - 0.4567 \frac{E_a}{RT} \quad (6)$$

where  $\alpha$  is the weight-loss ratio,  $A$  is frequency factor (s<sup>-1</sup>),  $R$  is ideal gas constant (8.314 J·mol<sup>-1</sup>·K<sup>-1</sup>). Figure 15(b) shows the graphs of thermal degradation kinetics data by Ozawa method. The formula can be deduced that  $\log \beta$  proportional to  $1/T_p$ , so we can calculated  $E_a$  by the slope ( $-0.4567E_a/R$ ).

Table 5 shows thermal degradation kinetics data of PDLA before and after chain extending.  $E_a$  obtained by both the methods was listed in Table 5. The  $E_a$  obtained from Ozawa and Kissinger methods were an approximate value, which indicated that two methods were can be very good to describe the thermal decomposition mechanism of PDLA before and after chain extending, on addition  $E_a$  of PDLA-MDI and PDLA-HDI were obviously higher than that of PDLA. The regression coefficient ( $R^2$ ) values obtained in the range of 0.9~0.999, for

both the methods further proved the applicability of these methods for predicting the thermal degradation behavior of PDLA before and after chain extending.<sup>29</sup> The results indicated that the effect of chain extender had enhanced  $E_a$  of thermal degradation of PDLA and significantly improved the thermal stability of PDLA.

## Conclusions

The purpose of this study was to evaluate the possibility of chain extending PDLA based on reactive extrusion process. The chain extended products were morphologically characterized and tested for mechanical performance and thermal properties. Results showed that the optimum conditions were found to be: PDLA-MDI (170 °C, 10 rpm, 5 wt%, 15 min); PDLA-HDI (170 °C, 10 rpm, 5 wt%, 10 min). <sup>1</sup>H NMR and FTIR analysis results confirmed the successful coupling reaction between the -NCO group of MDI and HDI with the -OH of PDLA. Tensile strength, elongation at break, and impact strength showed significant improvement.

Compared with pure PDLA, the crystallinity and thermal stability of chain extended PDLA were increased. SEM showed more shear zones and fibrillations the surfaces of PDLA-MDI and PDLA-HDI. Studies on chain extension reaction kinetics suggested the chain extension effect of HDI was better than that of MDI. The rheological results showed that the introduction of chain extender had improved the forces of molecular chains, and the mobility of PDLA chains was restricted. Meanwhile, the analysis of thermal degradation kinetic indicated that the effect of chain extender had improved the thermal stability by improving the thermal decomposition activation energy. In conclusion, MDI and HDI may eventually be used to chain extended PDLA based on reactive extrusion process.

**Acknowledgments:** Financial support from Key Laboratory Open Foundation (NO. 2016D03010) of Xinjiang Uygur Autonomous Region of China is greatly acknowledged.

## References

1. X. Deng, J. Hao, and C. Wang, *Biomaterials*, **21**, 22 (2001).
2. M. Martina and D. W. Huttmacher, *Polym. Int.*, **2**, 56 (2007).
3. J. E. Jang, H. Y. Kim, J. E. Song, D. Lee, S. Y. Kwon, J. W. Chung, and G. Khang, *Polym. Korea*, **37**, 669 (2013).
4. X. Xi, W. J. Zhen, S. Z. Bian, and W. T. Wang, *Polym. Korea*, **39**, 601(2015).
5. W. J. Zhen and J. L. Sun, *Polym. Korea*, **38**, 299 (2013).
6. W. Y. Jang, K. H. Hong, B. H. Cho, S. H. Jang, S. I. Lee, and B. S. Kim, *Polym. Korea*, **32**, 116 (2008).
7. T. Okihara, M. Tsuji, and A. Kawaguchi, *J. Macromol. Sci. Phys.*, **B30**, 119 (1991).
8. H. Yamane and K. Sasai, *Polymer*, **8**, 44 (2003).
9. X. F. Wei, R. Y. Bao, and Z. Q. Cao, *Macromolecules*, **4**, 47 (2014).
10. H. Li and M. A. Huneault, *Polymer*, **23**, 6855 (2007).
11. J. Cheng, J. Q. Sun, K. Wu, and X. L. Yun, *J. Chem. Eng. (in Chinese)*, **27**, 5 (2006).
12. C. Liu, Y. Jia, and A. He, *Int. Polym. Proc.*, **2013**, 1 (2013).
13. S. I. Woo, B. O. Kim, H. S. Jun, and H. N. Chang, *Polym. Bull.*, **35**, 415 (1995).
14. W. J. Zhen, J. Li, and Y. Xu, *Polym. Compos.*, **35**, 1023 (2014).
15. S. H. Lee, D. Kim, J. H. Kim, D. H. Lee, S. J. Sim, J. D. Nam, H. Kye, and Y. K. Lee, *Polym. Korea*, **28**, 519 (2004).
16. M. E. Hyun and S. C. Kim, *Polym. Eng. Sci.*, **28**, 743 (1988).
17. J. L. Espartero, I. Rashkov, S. M. Li, N. Manolova, and M. Vert, *Macromolecules*, **29**, 3535 (1996).
18. T. Kasuga, Y. Ota, M. Nogami, and Y. Abe, *Biomaterials*, **1**, 19 (2000).
19. P. J. Jandas, S. Mohanty, and S. K. Nayak, *J. Clean. Prod.*, **52**, 392 (2013).
20. C. S. Yoon and D. S. Ji, *Polym. Korea*, **33**, 581 (2009).
21. B. H. Li and M. C. Yang, *Polym. Adv. Technol.*, **17**, 439 (2006).
22. S. Y. Gu, M. Yang, T. Yu, T. Ren, and J. Ren, *Polym. Int.*, **7**, 982 (2008).
23. D. Battegazzore, S. Bocchini, and A. Frache, *Express Polym. Lett.*, **5**, 849 (2011).
24. D. J. Garlotta, *Polym. Environ.*, **9**, 63 (2001).
25. L. Jiang, J. Zhang, and M. P. Wolcott, *Polymer*, **48**, 7632 (2007).
26. Y. Liu, S. C. Li, and H. Liu, *Polym. Plast. Technol. Eng.*, **52**, 841 (2013).
27. H. E. Kissinger, *Anal. Chem.*, **29**, 1702 (1957).
28. T. Ozawa, *J. Thermal Anal.*, **2**, 301 (1970).
29. K. Chrissafis, *Thermochim. Acta.*, **1**, 511(2010).